

CONTENTS

	<i>Page</i>	
ABSTRACT	iii	1/A5
INTRODUCTION	1	1/A7
AIRBORNE SAR OVERFLIGHTS	2	1/A8
FRIM SAR SYSTEM AND PROCESSING	6	1/A12
DATA ANALYSIS	8	1/A14
DISCUSSION	11	1/B3
CONCLUSION	13	1/B5
ACKNOWLEDGMENTS	14	1/B6
REFERENCES	15	1/B7

JAN 31 1979

Item 830-H-15

NAS 1.60:1404

NASA Technical Paper 1404

Preliminary Results of SAR Soil Moisture Experiment, November 1975

B. J. Choudhury, A. T. C. Chang,
V. V. Salomonson, T. J. Schmugge,
and J. R. Wang

COMPLETED
ORIGINAL

JANUARY 1979

NASA

23

NASA Technical Paper 1404

Preliminary Results of SAR Soil Moisture Experiment, November 1975

B. J. Choudhury
Computer Sciences Corporation
Silver Spring, Maryland

A. T. C. Chang, V. V. Salomonson,
T. J. Schmugge, and J. R. Wang
Goddard Space Flight Center
Greenbelt, Maryland



National Aeronautics
and Space Administration

**Scientific and Technical
Information Office**

1979

This document makes use of international metric units according to the Systeme International d'Unites (SI). In certain cases, utility requires the retention of other systems of units in addition to the SI units. The conventional units stated in parentheses following the computed SI equivalents are the basis of the measurements and calculations reported.

ABSTRACT

This report presents preliminary results of the soil-moisture remote sensing experiment of November 1975, using a synthetic aperture radar (SAR) system. The experiment was performed using the Environmental Research Institute of Michigan's (ERIM) dual-frequency and dual-polarization side-looking SAR system on board a C-46 aircraft. The operating frequencies were 1.304 GHz (23 cm, L-band) and 9.375 GHz (3.2 cm, X-band). For each frequency, horizontally polarized pulses were transmitted and both horizontally and vertically polarized return signals were recorded on the signal film simultaneously. The test sites were located in St. Charles, Missouri; Centralia, Missouri; and Lafayette, Indiana. Each test site was a 4.83-km by 8.05-km (3-mile by 5-mile) rectangular strip of terrain. Concurrent with SAR overflight, ground soil samples of 0-to-2.5-cm and 0-to-15-cm layers were collected for soil moisture estimation. The surface features were also noted. Hard-copy image films and the digital data produced via optical processing of the signal films are analyzed in this report to study the relationship of radar backscatter to the moisture content and the surface roughness. Many difficulties associated with processing and analysis of the SAR imagery are noted. In particular, major uncertainty in the quantitative analysis appeared due to the difficulty of quality reproduction of digital data from the signal films.

Blank

Page

PRELIMINARY RESULTS OF SAR SOIL MOISTURE EXPERIMENT, NOVEMBER 1975

B. J. Choudhury

Computer Sciences Corporation

Silver Spring, Maryland

and

A. T. C. Chang, V. V. Salomonson, T. J. Schmugge,

and J. R. Wang

Laboratory for Atmospheric Sciences

Goddard Space Flight Center

Greenbelt, Maryland

INTRODUCTION

Measurement of soil moisture by remote sensing techniques has a number of applications in the fields of hydrology, meteorology, and agriculture. In the field of hydrology, knowledge of soil moisture is important for predicting the runoff following a rainstorm. Measurement of the soil moisture is necessary for the large-scale assessment of the transport of moisture flux into the atmosphere. The moisture content in the surface layer of an agriculture field is crucial to the successful germination and early growth of plants, and hence knowledge of this parameter helps to estimate eventual yield. Remote sensors at aircraft or satellite altitudes could potentially meet these measurement needs and adequately provide ground soil moisture information over a large area on a timely basis. Considerable work has been done using both passive and nonimaging active microwave sensors to remotely determine the soil moisture content at ground levels and at aircraft and satellite altitudes (References 1 to 4). However, the spatial resolutions of these sensors are usually limited by the practical size of the antennas. At satellite altitudes, these sensors would be useful in those applications only where a fine resolution is not required. To obtain a microwave image with a fine spatial resolution at satellite altitudes, a synthetic aperture radar (SAR) system must be considered.

The technique of using a synthetic aperture radar for remote sensing of the Earth's environment is not new. Schaber, Berlin, and Brown (Reference 5) used the Jet Propulsion Laboratory (JPL) airborne SAR to study the relationship between geological features and radar backscatter. The potential of using SAR imagery for open water and vegetation mapping was put forth by Drake and Shuchman (Reference 6). Blanchard (Reference 7) reported the possibility of using SAR imagery to improve runoff prediction. However, the first and only

attempt to quantitatively correlate airborne SAR imagery directly with soil moisture content came from the work of Cihlar, Ulaby, and Mueller (Reference 8). Although these authors showed a correlation between the radar return and soil moisture for a few selected fields, the results were in general inconclusive.

This document describes another attempt to assess the utility of SAR imagery for studying the relationship between radar return and soil moisture. The SAR used in the aircraft flights was the one operated by the Environmental Research Institute of Michigan (ERIM) (Reference 9). Three test sites of relatively flat terrain were chosen for the SAR overflights. The soil moisture ground truth measurements were made on a number of bare fields in each of the test sites (Reference 10). The radar returns from those fields were analyzed and studied in relation to moisture content and surface roughness. Many difficulties associated with the processing and analysis of SAR imagery were noted, but the results still indicate some potential for applying the SAR approach for soil moisture determination if these difficulties can be overcome.

AIRBORNE SAR OVERFLIGHTS

The test sites selected for the SAR overflights were located in St. Charles, Missouri; Centralia, Missouri; and Lafayette, Indiana. Each test site was a 4.83-km by 8.05-km (3-mile by 5-mile) rectangular strip of relatively flat terrain. The locations of these test sites are shown in figures 1, 2, and 3. Although other land-use categories were present, most of the land within these test sites consisted of agricultural fields. There were a reasonable number of bare fields in the test sites which were suitable for the soil moisture mission.

The ERIM SAR was mounted on a C-46 aircraft and flown over all three test sites on November 10, 1975. Each site was imaged by flying over the southern edge of the rectangle. This mode of operation provided low incident angles for most of the fields from which the ground truth data were collected. Aluminum reflectors were installed at several ground locations to provide spots of high-intensity return on the SAR imagery. These spots would later serve to facilitate field identification and registration. The altitudes of the aircraft and the estimated depression angles covered by the SAR were supplied by ERIM and are listed in table 1. A cold front passed through the St. Charles area on November 9, 1975. As a result, all the fields in that test site were wet during the SAR flight. The intensities of the radar backscattered signals were recorded in real time on the signal film aboard the aircraft.

The ground truth measurements of all three test sites were made on the same day of the SAR flights. The moisture contents of soils were measured at 0-to-2.5-cm and 0-to-15-cm depths for a number of selected fields (Reference 10). The surface features and conditions of those selected fields were noted. Color pictures both at ground level and at aircraft

**Microfilmed From
Best Available Copy**

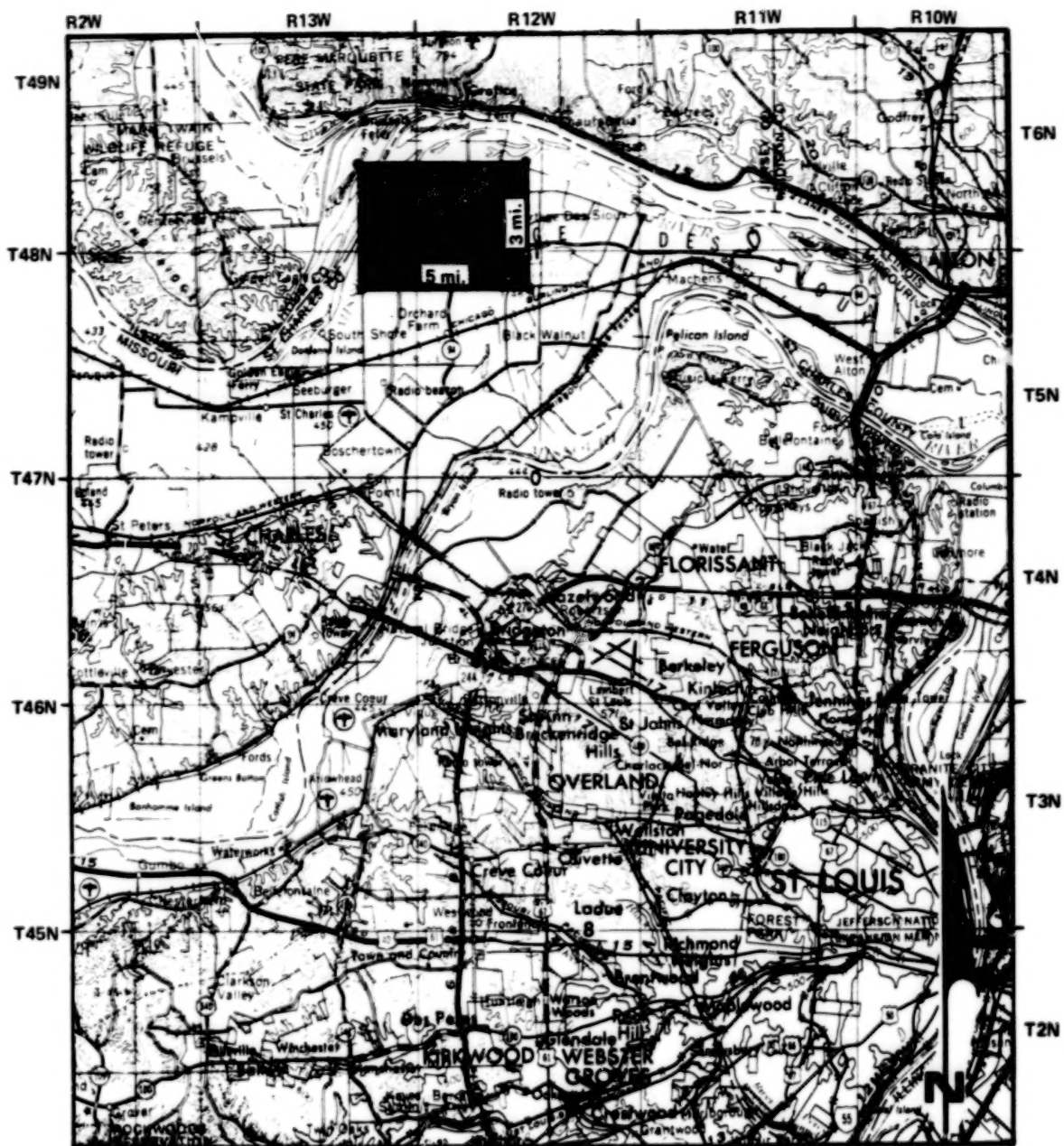


Figure 1. Test sites selected for the SAR overflights, St. Charles, Missouri (scale: 1 inch = 4 miles).

Microfilmed From
Best Available Copy

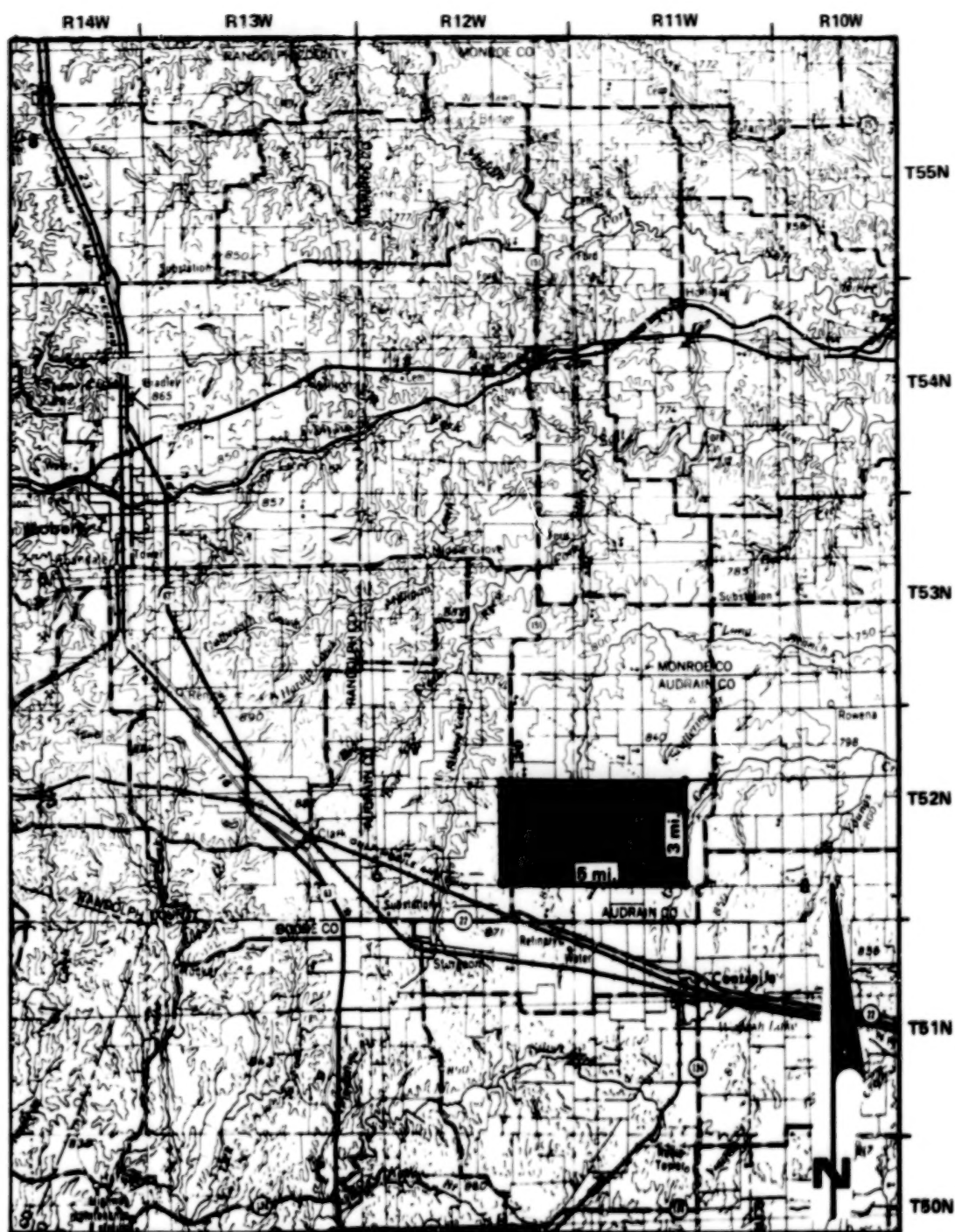


Figure 2. Test sites selected for the SAR overflights, Centralia, Missouri (scale: 1 inch = 4 miles).

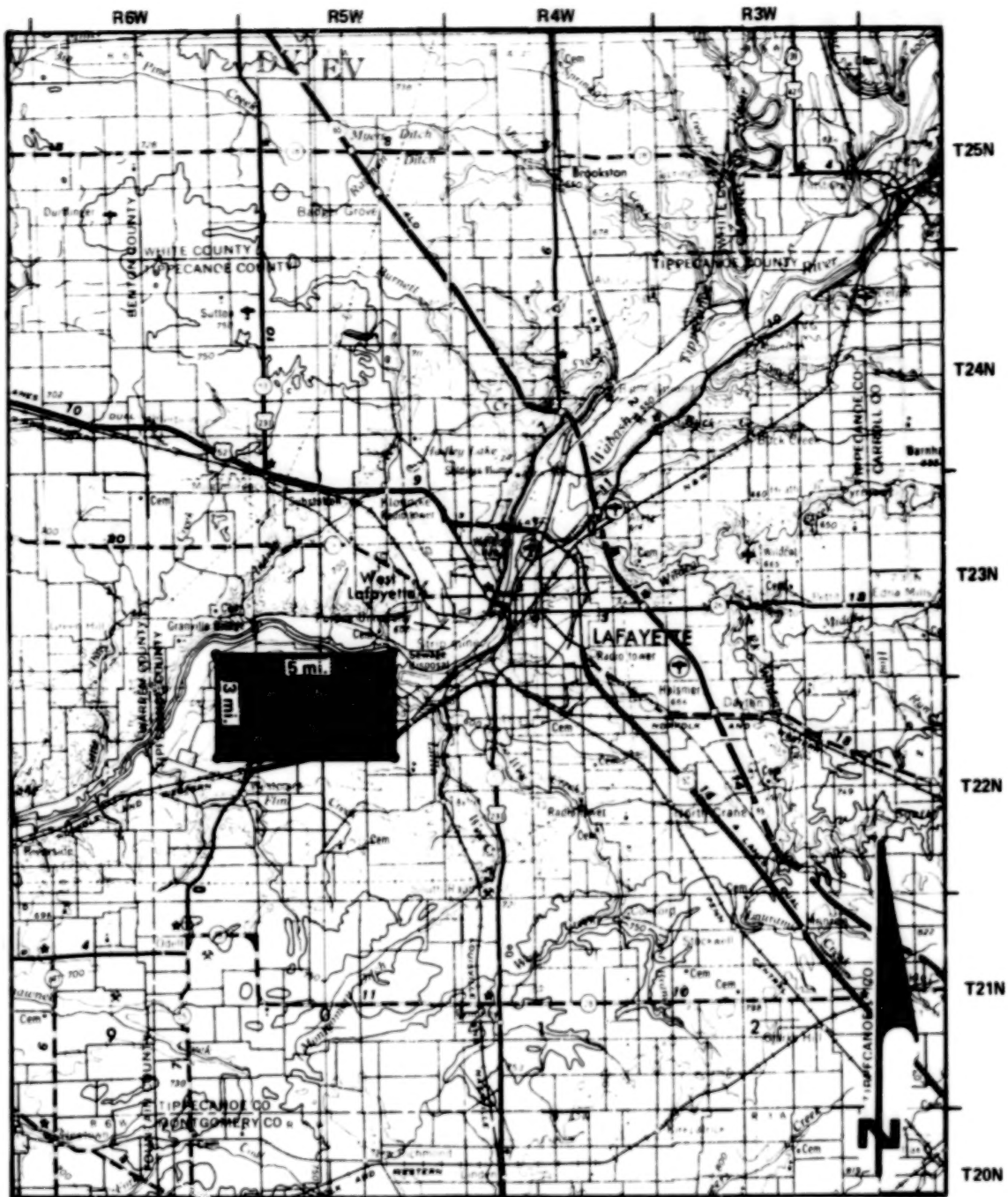


Figure 3. Test sites selected for the SAR overflights, Lafayette, Indiana (scale: 1 inch = 4 miles).

Table 1
Altitudes and Display Ranges

Site (average elevation)	Altitude	Slant Range	Estimated Depression Angle	
			Near Edge	Far Edge
Lafayette (179 m)	3940 m	3760 m	90°	24.1°
St. Charles (130 m)	3940 m	3240 m	90°	26.2°
Centralia (256 m)	3940 m	3730 m	90°	23.9°

altitudes were also taken for a majority of the fields. Both the field descriptions and the color pictures helped identify the locations of the fields in the data analysis. They also served as a basis for the approximate classification of the fields into categories of smooth, medium-rough, and rough surfaces. This approximate field classification was necessary in view of the dominant role played by the surface roughness parameter in the radar intensity return (Reference 3).

ERIM SAR SYSTEM AND PROCESSING

The ERIM SAR is a dual-frequency, dual-polarization, side-looking radar system. The operating frequencies are 1.304 GHz (23 cm, L-band) and 9.375 GHz (3.2 cm, X-band) (Reference 9). For each frequency, horizontally polarized pulses are transmitted. In this experiment, both horizontally and vertically polarized return signals were recorded on the signal film simultaneously. These dispersed signals are optically compressed so that the spatial dimension of the output signal is linearly proportional to the slant range of the terrain. The compressed signal film is then processed in an optical correlator at ERIM to produce either image film or digital data using an image dissector (Reference 11). Since the radar return in the cross polarization (HV) is generally much weaker than that in the like polarization (HH), the light-source intensities of the optical correlator may have to be set differently for the two polarizations to bring about the best contrast in both radar images. In this particular mission, the light source on the optical bench was increased to maximum intensity for the processing of the HV data. This increase in light-source intensity essentially shifted the level of the HV radar return up by approximately 5 dB relative to the level of the HH radar return. After these adjustments, adequate contrast among the fields on the image films were obtained for both polarizations.

A problem, to date, associated with the data reproduction scheme described in the preceding paragraph has been the lack of a standardized procedure. The ERIM optical correlator is

not a fully automatic system. The output product from that system may vary due to instrument drift or even due to different operators. An operator must make numerous manual adjustments on elements of the optical system to optimize the image from the recorded signal film. Some minor adjustments can affect the end-products considerably. Therefore the repeatability of quality end-products depends very much on the adjustments made by the operator.

The effect of the lack of a standardized procedure in data reproduction was evidenced in the analysis of the data delivered by ERIM. Two separate sets of the digital data were produced at two different times by ERIM from the same original signal film recorded over the test sites. By comparing the intensities of the two digital data sets over many fields, certain distinct differences were recognized. These differences were not a constant shift in intensity level from one set of data to another and were difficult to explain. After several conversations with ERIM personnel, concerning the matter, it is believed that difficulty in setting up the proper Doppler cutoff in the processing may have contributed to this inconsistency.

Due to expense, the digital data provided by ERIM were not compensated for the range distortion and the antenna-gain-pattern variation as a function of the depression angle. The antenna gain pattern for the SAR system was obtained by ERIM by flying repeatedly over a known target. Since this type of calibration is expensive and adequate measurements are difficult to obtain, the number of calibration points in the antenna pattern were limited. As a typical example of the SAR antenna pattern, figure 4 plots the measured data points for the L-band horizontal polarization provided by ERIM.

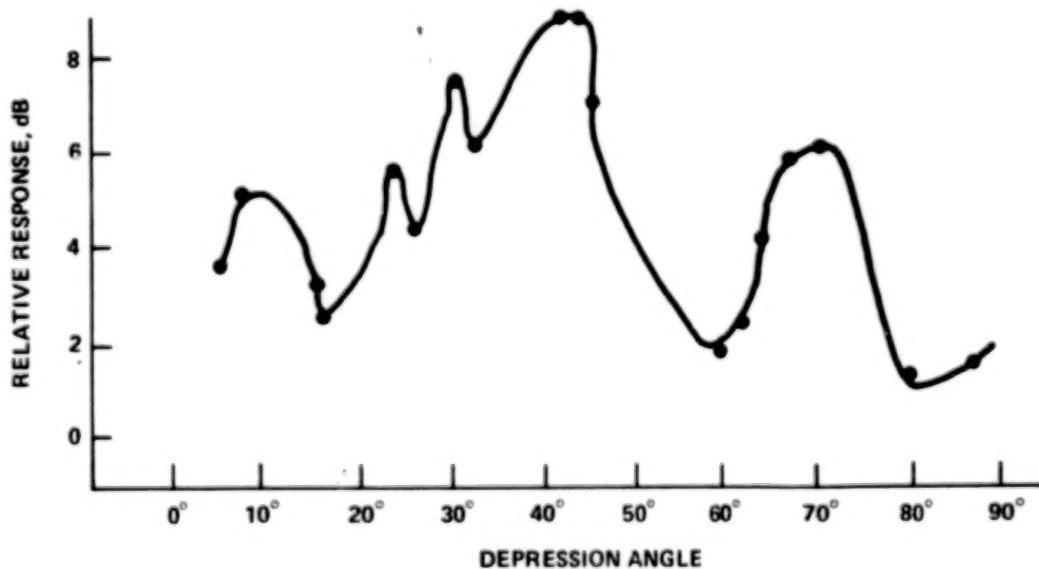


Figure 4. Data points for L-band horizontal polarization provided by ERIM.

DATA ANALYSIS

The SAR data were delivered to Goddard Space Flight Center (GSFC) in the forms of both the image films and the digital tapes. Different analysis procedures were applied to the image films and the digital tapes and are given in detail below. The following analysis and discussion will be limited mainly to the L-band HH polarization data for the test site in St. Charles, Missouri. Data for the other frequency/polarization and test sites will be mentioned only when necessary.

Analysis of the Digital Tape

As a first step in correlating the radar return intensity with the ground scene, a computer printout map was generated from the digital tape. There were a total of 38 alphanumeric characters used in the map. Each of these characters represented a small range of the radar return intensity. This range was adjusted to obtain the best contrast among the adjacent fields so that the ground control locations (road crossing, bridge, etc.) could be readily identified. After the desired contrast of the radar image was achieved, the next step was to obtain the coordinates of the boundaries for the fields where the ground truth measurements were made. To do this, several ground control points were selected and located on the printout map. The line numbers in both the along-track and the cross-track directions for those control points were recorded readily. The locations of the control points in the cross-track direction had to be calculated by the following formulas because of the image distortion inherent in the synthetic aperture radar technique. From figure 5, the incident angle θ is related to the height of the aircraft h and the cross-track line number N , measured from the near edge, by

$$\cos \theta = \frac{h}{h + NI} \quad (1)$$

where I is the cross-track ground distance per line in the printout map. If the printout map contains a total of M lines in the cross-track direction for the test site in which the maximum slant range is R_{\max} , then

$$I = \frac{R_{\max} - h}{M} \quad (2)$$

The distance x measured from the near edge and the cross-track line number in the printout map are related by

$$\begin{aligned} x &= h \tan \theta \\ &= h \tan \left(\cos^{-1} \left(\frac{hM}{(M - N)h + NR_{\max}} \right) \right) \end{aligned} \quad (3)$$

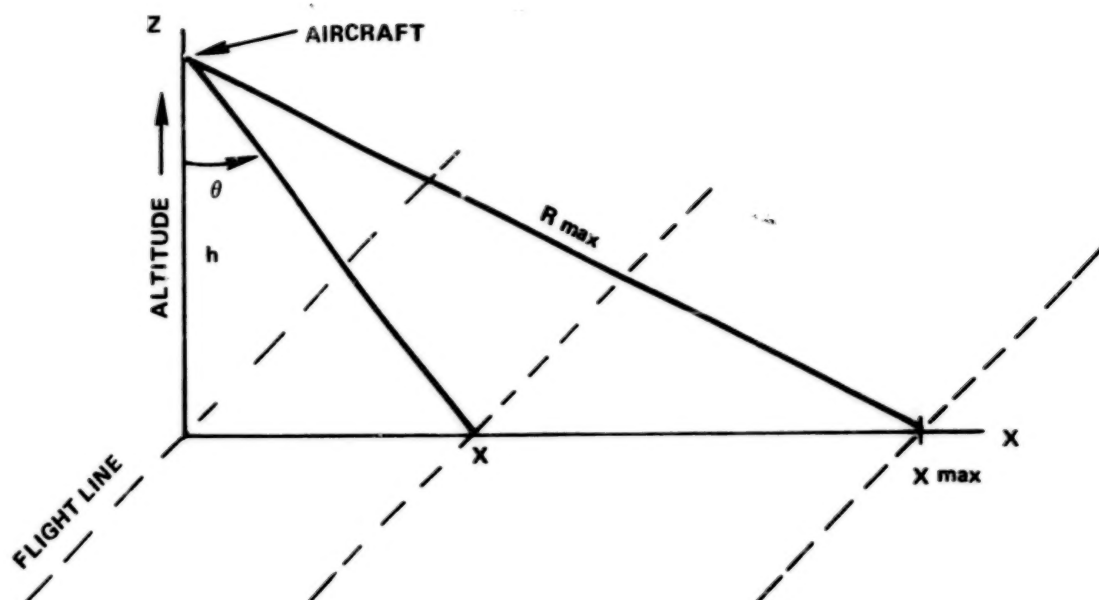


Figure 5. SAR data strip geometry.

Knowing the line number, the cross-track distance for each of the ground control points was calculated from equation 3 and was cross-checked using the geographic map of the test sites. The resolution of each line on the printout map in the along-track direction could be estimated in the process. The locations of the ground control points were then used along with the tone-change criteria to identify the fields on the printout map. Once a particular field was identified, the rows and columns of the field boundary on the printout map were noted. After all the fields for which ground truth data were collected were thus identified at a test site, the boundary coordinates were used as the control parameters to calculate the mean and standard deviations of the radar return intensity for each of the fields. It was found that although all four radar images (dual frequency and dual polarization) were recorded simultaneously on the signal film, the four sets of boundary coordinates for a given field determined by the above procedures from the printout maps were generally not identical. As a result, the field boundaries had to be calculated separately for each of the four radar images. To eliminate the possible effect of the field boundary on the mean and standard deviations of the radar return, the data points within a narrow strip along the boundary were excluded from the calculations.

There were a total of 25 bare fields in the St. Charles test site from which the ground truth data were taken. Out of these 25 fields, 9 were located close to the near edge between the nadir and the incidence angle of 15° . The SAR imagery in that region was so compressed that a unique identification of the individual fields was virtually impossible, and therefore was not done. The remaining 16 fields could be uniquely identified from the SAR imagery. The mean radar return for each of these 16 fields was normalized to field no. 9, which has the highest return, and listed in tables 2a and 2b. Fields with incident angles within 15 to 20° are given in table 2a, while those within 35 to 40° are given in table 2b. The corresponding average soil moisture content in the top 2.5-cm layer and the field description are also included in the tables. Based on the field descriptions and the photographs taken of the test site during the mission, these 16 fields could be approximately grouped into three categories according to the surface roughness. They are: (1) very rough surface due to rough plowing—fields no. 4, 5, 6, 16, and 18 belong to this category; (2) medium-rough surface, which were plowed and disced—fields no. 10, 11, 13, 14, 15, 17, and 22 belong to this category; and (3) smooth surface, which were smoothly disced—fields no. 9, 12, 19, and 20 belong to this category. The field classification is indicated in tables 2a and 2b by S, M, and R for smooth, medium-rough, and rough surfaces, respectively.

Analysis of Image Films

In order to compare the qualities of the SAR data represented in digital form and image form, the SAR image films were digitized and were processed by the Atmospheric and Oceanographic Information Processing System (AOIPS) at GSFC. Since this system requires data input in digital form, the films were digitized and the digitized data stored on magnetic tape by the General Electric Image-100 system located in Beltsville, Maryland. For each segment of the image film digitized, the digitizer was adjusted to obtain the maximum dynamic range for the film gray-scale variations. The AOIPS then produced from the digital tape the tone-contrast visual image in black and white on a cathode-ray tube. The control points, as well as the fields for which the ground truth measurements were made, were identified from the visual image. The built-in software in the system was then used to calculate the mean and standard deviations for each field. The average radar returns from all the identified fields were again normalized to that of field no. 9. The normalized radar return for each field was also entered in tables 2a and 2b. Field no. 20 was small in size and had an incidence angle close to 15° . It could not be identified from the image film, and therefore its entry in table 2a is missing.

The examinations of the image films revealed a possible effect of air turbulence on the SAR operation. The X-band image films for both polarizations obtained for the test site at Lafayette, Indiana, showed bands of wavy features. The L-band image films for the same test site did not show these features. The presence of these bands made the derivation and interpretation of the field radar return difficult. The effect of air turbulence is likely to remain a problem for the short-wavelength SAR.

Table 2a
Relative Radar Return, Soil-Moisture Content, and Surface Description
for Sampled Fields (Incidence Angle 15 to 20°)

Field No.	Soil Moisture, Percentage	Relative Radar Return (dB)		Surface Description
		Digital Data	Image Film	
4	35.5	-3.9	-4.0	Rough plowed
5	39.8	-2.7	-2.8	Rough plowed
6	34.3	-1.6	-2.8	Rough plowed
9	32.2	0	0	Plowed, relief lost due to weathering
13	25.2	-0.2	-0.2	Plowed and slightly disced
19	25.6	-3.9	-4.2	Disced
20	19.9	-6.0	—	Smoothly disced
22	25.5	-1.1	-0.1	Plowed and disced

DISCUSSION

An examination of tables 2a and 2b immediately shows that there are discrepancies in the radar intensity returns derived from the two forms of SAR data. For the fields with incident angles between 15 and 20°, the differences in the radar returns calculated from the two data sets were generally small, the largest difference being about ~1.3 dB. For those fields between 35 and 40°, the radar returns obtained from the image film were several decibels higher than those directly derived from the digital tape. Those discrepancies are probably due to: (1) the lack of dynamic range in the film product, (2) the gain drifts in the digitizer, or both. A similar problem in working with the image films might have existed in the results of Schaber et al. (Reference 5). Those authors studied the radar returns from terrains of varying roughness in the Death Valley, California, area by the JPL airborne SAR at a wavelength of 25 cm. They analyzed the SAR image film for the area at a particular incident angle of 40° and found a ~5-dB drop in the radar return from an extremely rough surface to a smooth, flat surface. On the other hand, a National Aeronautics and Space Administration (NASA)/Johnson Space Center (JSC) airborne L-band scatterometer flight over the same general ground location showed a drop of radar return, at the same incident angle, of ~15 dB from the rough to smooth terrain surfaces (S. C. Reid, personal communication).

Table 2b
Relative Radar Return, Soil-Moisture Content, and Surface Description
for Sampled Fields (Incidence Angle 35 to 40°)

Field No.	Soil Moisture, Percentage	Relative Radar Return (dB)		Surface Description
		Digital Data	Image Film	
10	42.8	- 5.3	-2.4	Plowed field with stubble
11	30.9	- 5.3	-1.2	Plowed and disced
12	37.2	- 8.2	-5.2	Corn stubble with emerging vegetation
14	32.3	- 4.8	-2.2	Plowed and disced
15	27.2	-10.2	-6.2	Plowed and disced
16	31.8	- 2.7	-1.8	Rough plowed
17	26.6	- 4.5	-1.8	Disced
18	27.1	- 6.9	-3.2	Plowed

Although the JSC scatterometer is operated at the wavelength of ~ 18 cm, it is not likely that the small difference in the operational wavelengths would result in a ~ 10 -dB difference in the radar intensity return.

As a result of a cold front passing through the St. Charles, Missouri, area, 0.64 cm of rain fell 1 day before the SAR flight, and all the fields in this test site had high moisture contents. The fields listed in tables 2a and 2b showed a soil moisture range from about 20 to 43 percent by dry weight. Fields no. 19 and 20 are composed of Logiois loam with 3 to 8 percent surface slopes. The rest of the fields were made of Warsaw loam with 0 to 3 percent surface slopes.

The small number of bare fields, the poor knowledge of the SAR antenna pattern variations, and the large effect due to surface roughness make it difficult to analyze the data quantitatively and derive a conclusive relationship between the soil moisture content and the radar return. However, a qualitative relation between the surface roughness and the radar return is present from the data in the tables. As an example, for the fields with incident angles between 35 and 40° with moisture content greater than 30 percent, field no. 16 of the rough surface category had the highest return, -2.7 dB. The medium-rough fields, nos. 10,

11, 14, and 15, gave an averaged radar return of -5.5 dB. Smooth field no. 12 had a low return of -8.2 dB. Among those fields with incident angles between 15 and 20° and with moisture content greater than 30 percent, smooth field no. 9 had a radar return about 2.5 dB higher than the average of the radar returns from rough fields no. 4, 5, and 6. These features are generally consistent with the results for the truck-mounted radar measurements (Reference 3). A comparison between smooth fields no. 9 and 20 showed a ~6-dB difference in the measured radar return. This difference could be related to the different moisture contents in the two fields.

Clearly, the results presented above do not offer much improvement in the relationship between soil moisture content and the SAR data output compared to those already reported by Cihlar et al. (Reference 8). However, several difficulties encountered in the data analysis might turn out to be valuable in the future. For example, the poor knowledge of the antenna gain pattern may not prevent the SAR from being a good mapping device for the delineation of scenes with very different natures (e.g., between land and water or between sea ice and water). For the remote sensing of ground soil moisture content where the radar sensitivity is ~0.3 dB/0.01 g/cm³ (Reference 12), more precise measurements of the SAR antenna gain pattern would be required. Another obvious difficulty comes from the very crude roughness classification of the fields in the test site. Since roughness is a crucial parameter affecting the radar backscatter, a better classification scheme would be necessary. Other difficulties are included in the following summary.

CONCLUSION

The microwave images obtained by ERIM SAR have been analyzed for the radar response to the changes of both soil moisture content and surface roughness. The analysis was performed on the data given in the forms of both digital tapes and image films. The small number of fields with ground truth measurements, the lack of precise surface roughness description of the fields, and the poor knowledge of the antenna pattern presented difficulties in analyzing the data quantitatively. However, a qualitative analysis of the data showed the variation of radar response to the surface roughness generally consistent with the results of the truck-mounted radar measurements. More importantly, the present study has brought to attention the following problems which will affect the future applications of the SAR system in the remote sensing of soil moisture: (1) The digital data varied according to the different laboratory setup in the optical processor. In order to acquire a repeatable data set, a direct digital processor is required. (2) The external calibration technique used is not adequate for soil moisture determination. An internal closed-loop calibration procedure should be developed to provide a good calibration for the return signal. Without accurate calibration, it will be impossible to detect any temporal soil moisture variations. (3) Precise measurements of the antenna gain pattern should be made so that the SAR imagery can be

compensated for the antenna pattern effect. The effect of radome and antenna side-lobe contribution should be studied carefully before experimental data can be analyzed to obtain any meaningful results. (4) Air turbulence has considerable effect on the phase coherence of the return signal. The synthetic aperture radar system's image quality would be limited by severe weather conditions. (5) A better surface roughness classification scheme should be defined. The present classification method based on photographs and field description probably is not sufficient for a soil moisture estimation by SAR. (6) The information contained in the ERIM SAR imagery between the near edge up to a 15° incident angle was impossible to extract. Nevertheless, the results suggest that, if these data acquisition difficulties can be overcome, the inherent capability of the SAR approach to provide high spatial, nearly all-weather observations from satellite altitudes, call for further efforts to develop relationships between SAR observations to soil moisture and other moisture-related parameters such as vegetation biomass and snowpack properties.

ACKNOWLEDGMENTS

The authors wish to express their thanks to R. Larson of ERIM for many useful discussions and to B. Jones and his associates of the Resources Consultations, Inc. (formerly M. W. Bittinger & Associates, Inc.), for their assistance in collecting ground truth information.

Goddard Space Flight Center
National Aeronautics and Space Administration
Greenbelt, Maryland October 1978

REFERENCES

1. Newton, R. W., "Microwave Remote Sensing and Its Application to Soil Moisture Detection," Technical Report RSC-81, Texas A&M University, College Station, January 1977.
2. Schmugge, T., "Remote Sensing of Surface Soil Moisture," *2nd Conf. on Hydrometeorology*, Publ. American Meteorological Society, Boston, Massachusetts, October 1977, pp. 304-310.
3. Batlivala, P. P., and F. T. Ulaby, "Estimation of Soil Moisture with Radar Remote Sensing," *Proc. 11th Intern. Symp. on Remote Sensing Environment*, Vol. 2, 1977, pp. 1557-1566.
4. Eagleman, J. R., "Moisture Detection from Skylab," *Ninth Intern. Symp. Remote Sensing Environment*, Ann Arbor, Michigan, 1974, pp. 701-705.
5. Schaber, G. G., G. L. Berlin, and W. E. Brown, Jr., "Variations in Surface Roughness within Death Valley, California: Geologic Evaluation of 25-cm-Wavelength Radar Images," *Geological Society of America Bulletin*, Vol. 87, January 1976, pp. 29-41.
6. Drake, B., and R. A. Shuchman, "Feasibility of Using Multiplexed SLAR Imagery for Water Resources Management and Mapping Vegetation Communities," *Proc. 9th Intern. Symp. Remote Sensing Environment*, Ann Arbor, Michigan, Vol. 1, 1974, pp. 219-250.
7. Blanchard, B. J., "Analysis of Synthetic Aperture Radar Imagery," Final Report RSC2359-2, Texas A&M University, College Station, Texas, June 1977.
8. Cihlar, J., F. T. Ulaby, and R. Mueller, "Soil Moisture Detection from Radar Imagery of the Phoenix, Arizona Test Site," RSL Technical Report 264-4, University of Kansas, Lawrence, June 1975.
9. Rawson, R., and F. Smith, "Four Channel Simultaneous X and L Band Imaging SAR Radar," *Proc. 9th Intern. Symp. Remote Sensing Environment*, Vol. 1, Ann Arbor, Michigan, 1974, pp. 251-270.

10. Jones, E. B., and S. E. Olt, "Soil Moisture Ground Truth, November 10, 1975 Mission," M. W. Bittinger & Associates, Inc., December 1975.
11. Bayma, R. W., R. L. Jordon, and B. N. Manning, "A Survey of SAR Image-Formation Processing for Earth Resources Applications," *Proc. 11th Intern. Symp. Remote Sensing Environment*, Vol. 1, Ann Arbor, Michigan, April 1977, pp. 137-159.
12. Batlivala, P. P., and F. T. Ulaby, "Remotely Sensing Soil Moisture with Radar," RSL Technical Report 264-8, University of Kansas, Lawrence, August 1976.

BIBLIOGRAPHIC DATA SHEET

1. Report No. NASA TP-1404	2. Government Accession No.	3. Recipient's Catalog No.	
4. Title and Subtitle Preliminary Results of SAR Soil Moisture Experiment, November 1975		5. Report Date January 1979	
		6. Performing Organization Code 913	
7. Author(s) B. J. Choudhury, A. T. C. Chang, T. J. Schmugge, V. V. Salomonson, and J. R. Wang		8. Performing Organization Report No. G7802-F21	
9. Performing Organization Name and Address Goddard Space Flight Center Greenbelt, Maryland 20771		10. Work Unit No. 177-55-44	
		11. Contract or Grant No.	
12. Sponsoring Agency Name and Address National Aeronautics and Space Administration Washington, D.C. 20546		13. Type of Report and Period Covered Technical Paper	
		14. Sponsoring Agency Code	
15. Supplementary Notes			
16. Abstract This report presents preliminary results of the soil-moisture remote sensing experiment of November 1975, using a synthetic aperture radar (SAR) system. The experiment was performed using the Environmental Research Institute of Michigan's (ERIM) dual-frequency and dual-polarization side-looking SAR system on board a C-46 aircraft. The operating frequencies were 1.304 GHz (23 cm, L-band) and 9.375 GHz (3.2 cm, X-band). For each frequency, horizontally polarized pulses were transmitted and both horizontally and vertically polarized return signals were recorded on the signal film simultaneously. The test sites were located in St. Charles, Missouri; Centralia, Missouri; and Lafayette, Indiana. Each test site was a 4.83-km by 8.05-km (3-mile by 5-mile) rectangular strip of terrain. Concurrent with SAR overflight, ground soil samples of 0-to-2.5-cm and 0-to-15-cm layers were collected for soil moisture estimation. The surface features were also noted. Hard-copy image films and the digital data produced via optical processing of the signal films are analyzed in this report to study the relationship of radar backscatter to the moisture content and the surface roughness. Many difficulties associated with processing and analysis of the SAR imagery are noted. In particular, major uncertainty in the quantitative analysis appeared due to the difficulty of quality reproduction of digital data from the signal films.			
17. Key Words (Selected by Author(s)) SAR, Soil moisture, Surface roughness, AOIPS		18. Distribution Statement STAR Category 46 Unclassified-Unlimited	
19. Security Classif. (of this report) Unclassified	20. Security Classif. (of this page) Unclassified	21. No. of Pages 21	22. Price* \$4.00

END

APR 30 1979